Inorganic Chemistry

Article

pubs.acs.org/IC

Unusual Formation of a Stable 2D Copper Porphyrin Network

Anna A. Sinelshchikova,[†] Sergey E. Nefedov,[‡] Yulia Yu. Enakieva,[†] Yulia G. Gorbunova,*[,†,‡] Aslan Yu. Tsivadze,[†,‡] Karl M. Kadish,[§] Ping Chen,[§] Alla Bessmertnykh-Lemeune,[⊥] Christine Stern,[⊥] and Roger Guilard*[,⊥]

[†]Frumkin Institute of Physical Chemistry and Electrochemistry, Russian Academy of Sciences, Leninsky Pr. 31, Moscow 119071, Russia

[‡]Kurnakov Institute of General and Inorganic Chemistry, Russian Academy of Sciences, Leninsky Pr. 31, Moscow 119991, Russia

[§]Department of Chemistry, University of Houston, Houston, Texas 77204-5003, United States

[⊥]Université de Bourgogne, ICMUB (UMR CNRS 6302), 9 Avenue Alain Savary, BP 47870, 21078 Dijon Cedex, France

Supporting Information

ABSTRACT: Copper(II) 5,15-bis(diethoxyphosphoryl)-10,20-diphenylporphyrin was obtained and characterized by means of cyclic voltammetry, electron paramagnetic resonance, Fourier transform infrared, and UV−visible spectroscopy. Three crystalline forms were grown and studied by means of X-ray diffraction methods (single crystal and powder). The highly electron-withdrawing effect of phosphoryl groups attached directly to the porphyrin macrocycle results in a self-assembling process, with formation of a stable 2D coordination network, which is unusual for copper(II) porphyrins. The resulting 2D structure is a rare example of an assembly based on copper(II) porphyrins where the copper(II) central metal ion is six-coordinated because of a weak interaction with two phosphoryl groups of adjacent porphyrins. The other polymorph of copper(II) 5,15-bis(diethoxyphosphoryl)-10,20-diphenylporphyrin contains individual (isolated) porphyrin molecules with four-coordinated copper(II) in a distorted porphyrin core. This polymorph can be obtained only by slow diffusion of a copper acetate/methanol solution into solutions of free base 5,15-bis(diethoxyphosphoryl)-10,20-diphenylporphyrin in chloroform. It converts to the 2D structure after dissolution in chloroform followed by consecutive crystallizations, using slow diffusion of hexane. A six-coordinated copper(II) porphyrin containing two axially coordinated dioxane molecules was also obtained and characterized by X-ray diffraction crystallography. The association of copper(II) 5,15-bis(diethoxyphosphoryl)-10,20-diphenylporphyrin in solution was also studied.

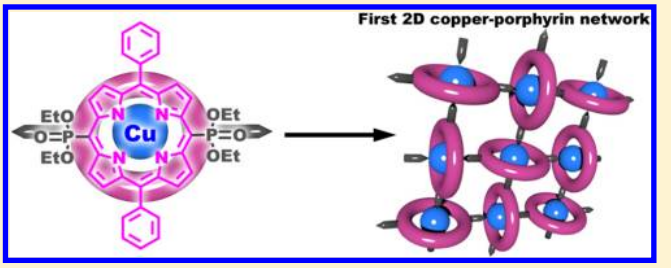

INTRODUCTION

Mimicking biological processes, which occur in living systems, is of great current interest. In this regard, synthetic metalloporphyrin assemblies have been widely studied because they are key functional systems for many biochemical processes.[1−9] Porphyrins and their metal complexes are important building blocks for self-organization of highly ordered assemblies that have different dimensionality and topology (1D, 2D, and 3D structures) because of their unique structural and coordination properties, thermal and chemical robustness, and rich physicochemical properties.[10−15] It is not easy to predict how exactly molecular building blocks will assemble in the solid state, but some tuning can be made by changing the peripheral functional groups, the ligand topology, and the nature of the metal center. The majority of known porphyrin self-assemblies have been formed from zinc porphyrins possessing nitrogen/oxygen-donor functional groups at the *meso*- or *β*-pyrrole positions of the macrocycle. The exceptional role of zinc ions in porphyrin assemblies relies on the simple metalation of functionalized porphyrins by zinc salts and the ability of zinc ions to coordinate one or two additional axial ligands, generating networks of different topologies.[16−24]

Copper porphyrins are easy to prepare under mild conditions. However, there are only a few examples of coordination polymers formed by copper(II) porphyrins. Indeed, copper(II) porphyrins are almost always composed of individual molecules in the solid state because of the preferred four-coordinated environment of copper(II) ions in these receptors.[25−31] External metal cations are often needed for assembling functionalized copper(II) porphyrins using coordinating groups at the porphyrin core. Thus, coordination polymers have been obtained by the reaction of copper(II) porphyrins with different metal salts, for example, $Cd(NO_3)_2$, $CuBr_2$, or $Cu(BF_4)_2$.[32−38]

The self-assembly of copper(II) porphyrins via internal metal centers is even more rare. To our knowledge, there is only one example in the literature for a 1D coordination polymer formed by the self-assembly of a copper porphyrin in which the

Received: October 15, 2012

   dx.doi.org/10.1021/ic302257g | Inorg. Chem. XXXX, XXX, XXX−XXX

copper(II) center adopts a distorted octahedral coordination environment.[39] Axial coordination of adjacent porphyrin molecules via the formation of Cu···N bonds for copper(II) *meso*-tetrakis(*o*-isonicotinoylamidophenyl)porphyrin in the solid state results in formation of the coordination polymer. Moreover, studies of copper porphyrin assemblies are of key importance for the modeling of biochemical processes because copper(II) is an essential metal cation found in enzymes, structural proteins, assimilation pigments, and different biological processes.[40−42] It was shown, for example, that the formation of a complex containing three metal copper(II) centers bound to a central phosphate unit bridging oxygen atoms and to a tripodal $N(CH_2\text{-}o\text{-}C_6H_4CH_2N(CH_2py)_2)_3$ ligand structurally mimics trimetallic active sites of proteins involved in phosphate metabolism.[43]

Our recent synthetic efforts have led to the development of porphyrins bearing diethoxyphosphoryl groups at two meso positions of the macrocycle (see, for example, compound **1** in Chart 1).[44,45]

Chart 1

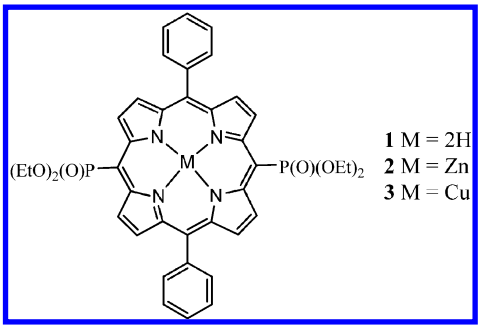

The electron-withdrawing nature of the diethoxyphosphoryl groups favors the self-assembly of a related zinc porphyrinate, **2**, both in the solid state and in solution.

In a continuation of our earlier studies of porphyrin **1** as a new building block,[44,45] we report here on the peculiarities of the coordination chemistry of copper(II) 5,15-bis-(diethoxyphosphoryl)-10,20-diphenylporphyrin (**3**) and provide the first example of a 2D coordination polymer formed by the self-assembly of copper porphyrin molecules (Chart 1).

RESULTS AND DISCUSSION

Synthesis and X-ray Study. Paddle-wheel dinuclear carboxylates of transition metals are well-known deprotonating agents,[46] and copper(II) carboxylate could be used as a metal source to obtain the copper(II) porphyrin **3** under mild conditions in the absence of additional base. Thus, slow diffusion of a $Cu(OAc)_2\cdot H_2O$/methanol solution ($c = 5.08 \times 10^{-3}$ M) into a stoichiometric amount, or a 4-fold excess, of the free base 5,15-bis(diethoxyphosphoryl)-10,20-diphenylporphyrin (**1**; 1.27×10^{-3} M) in $CHCl_3$ at room temperature over 2 days resulted in deprotonation of **1** and the formation of violet single crystals of **3** (Table 1, entry 1).

According to the X-ray data (Figure 1 and Tables S1 and S2 in the Supporting Information), the copper(II) ion in the crystals (**3a**) is located in the center of symmetry and adopts a distorted square-planar environment formed by four nitrogen atoms of the porphyrin macrocycle [Cu(1)−N(1/1A) = 2.005(3) Å; Cu(1)−N(2/2A) = 1.993(3) Å]. The angle between the Cu−N(1)−N(2) and Cu−N(1A)−N(2A) planes is 8.2°, and a displacement of the four pyrrole N_4 atoms from the mean porphyrin plane is within ±0.100 Å. The porphyrin macrocycle is significantly saddled, and the four pyrrole rings are considerably distorted in an alternant fashion, either upward or downward with respect to the mean N_4 plane. The displacement of carbon atoms from the macrocycle varies from −0.742 to +0.575 Å [maximum for C(17/17A)], values that are significantly larger than those in several structurally characterized *meso*-tetraaryl-substituted copper porphyrins.[25,30,31,47−51]

Copper atoms of the two closest molecules of **3a** in the crystal cell are located at a distance of 5.490 Å from each other (Figure S1 in the Supporting Information) and have relatively short atomic interactions with carbon atoms of the pyrrole fragment in the adjacent porphyrin molecule [Cu(1A/1B)−C(16B/16A) = 3.351 Å; Cu(1A/1B)−C(17B/17A) = 3.131 Å]. The atom C(16A/16B) is located 3.393 Å from the atom N(2D/2C), which probably influences distortion of the molecule. All other intermolecular contacts between the two closest molecules are much longer than 3.5 Å [the shortest ones are N(2A/2B)−C(18B)/(18A) = 3.562 Å, N(2A)−N(2B) = 3.611 Å, and $C_{porphA}-C_{porphB}$ = 3.886−3.911 Å].

Table 1. Crystal Growth Conditions for Polymorphs 3a and 3b and Solvate 3c

		solvent[a]			
entry	XRD structure of the porphyrin precursor	A	B	additive	single-crystal structure
1	**1**	$CHCl_3$	[b]		**3a**
2	**3b**	$CHCl_3$	hexane		**3b**
3	**3b**	$CHCl_3$	MeOH		**3b**
4	**3b**	$CHCl_3$/MeOH	hexane		**3b**
5	**3b**	$CHCl_3$	MeOH	AcOH	**3b**
6	**3b**	$CHCl_3$	MeOH	$Cu(OAc)_2$	**3b**
7	**3a**	$CHCl_3$	hexane		**3b**
8	**3b**	dioxane			**3c**

[a]The porphyrin precursor was dissolved in solvent A, and solvent B was used as a second phase in slow diffusion experiments. [b]A solution of $Cu(OAc)_2$ in MeOH was used as a second phase.

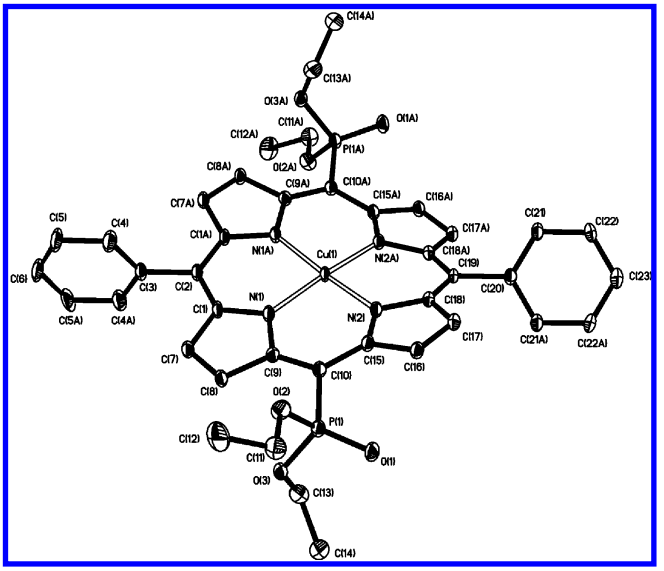

Figure 1. Molecular structure of complex **3a**. Displacement ellipsoids are drawn at the 50% probability level. Hydrogen atoms are omitted for clarity.

dx.doi.org/10.1021/ic302257g | *Inorg. Chem.* XXXX, XXX, XXX−XXX

The phenyl substituents at the meso positions of the macrocycle [C(2A)−C(3A) = 1.502(3) Å; C(19A)−C(20A) = 1.499(3) Å] have different twist angles toward the porphyrin plane [C(1A)−C(2A)−C(1C)/C(3A)−C(4A)−C(4C) = 88.1°; C(18A)−C(19A)−C(18C)/C(20A)−C(21A)−C(22C) = 54.9°]. This fact can be explained by steric contacts in the crystal packing between one of the phenyl rings and a pyrrole fragment of the adjacent porphyrin. The shortest distances are 3.440 and 3.520 Å from C(21A) or C(21B) to C(8B) or C(8A) and C(9B) or C(9A), respectively (Figure S1 in the Supporting Information).

The oxygen atoms of the two diethoxyphosphoryl substituents have no major interactions with other atoms of the molecule (Figure 2). Displacement of the phosphorus atom from the N_4 plane is ±0.286 Å, and the P(1)−C(10) distance is 1.806(3) Å. The P(1)−O(1) distance is 1.470(2) Å, P(1)−O(2) is 1.568(3) Å, and P(1)−O(3) is 1.585(3) Å. The dihedral angle between the C(9)−C(10)−C(15) and C(10)−P(1)−O(1) planes is 14.6°.

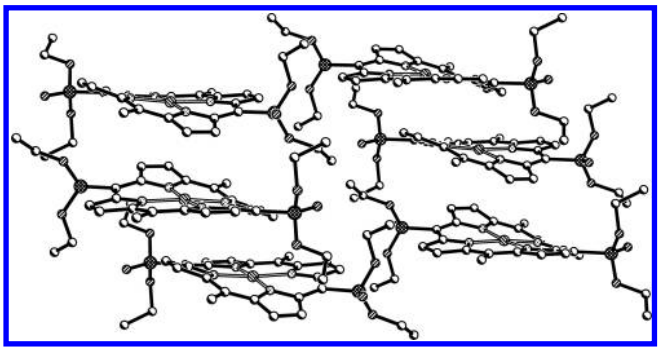

Figure 2. Crystal packing of **3a**. The hydrogen atoms and *meso*-aryl group are omitted for clarity except for the *ipso*-carbon atoms.

In contrast to the distorted porphyrin macrocycle in **3a**, the molecule of porphyrin **1** is almost planar, with displacement of the nitrogen atoms from the N_4 plane being ±0.012 Å (Figure 3). The dihedral angles of the phosphoryl substituents are 5.4° and 7.9° between the CCC−CP═O planes [the P−C distances are 1.808(2) and 1.813(2) Å, and the displacement values of the phosphorus atoms from the N_4 plane are −0.1496 and +0.5582 Å). With respect to the N_4 plane, which represents the mean plane of the porphyrin core, the twist angles of the aryl rings are 77.7° and 74.4°. The displacement of the *meso*-carbon and phenyl carbon atoms from the N_4 plane ranges from −0.108 to +0.089 Å, and the *meso*-C−C_{Ph} distance is 1.501 Å. In the crystal packing of the free base porphyrin **1**, there are no remarkable intermolecular contacts; this is because of the presence of two chloroform solvate molecules, which form hydrogen bonds with oxygen atoms of the phosphoryl substituents (P═O distance =1.467 Å; P−O distance = 1.565−1.584 Å; P═O···H_{CHCl_3} contacts are 2.143−2.150 Å).[45]

The preparative synthesis of **3** was monitored by UV−visible absorption spectroscopy and showed complete consumption of free base **1** after 30 min in a reaction with copper acetate monohydrate (ratio 1:3.5) in a $CHCl_3$/methanol solution (10:1, v/v) at room temperature. This led to the formation of a violet complex, which was isolated after purification by column chromatography (SiO_2 and eluent $CHCl_3$) in 91% yield. This complex was characterized by means of matrix-assisted laser

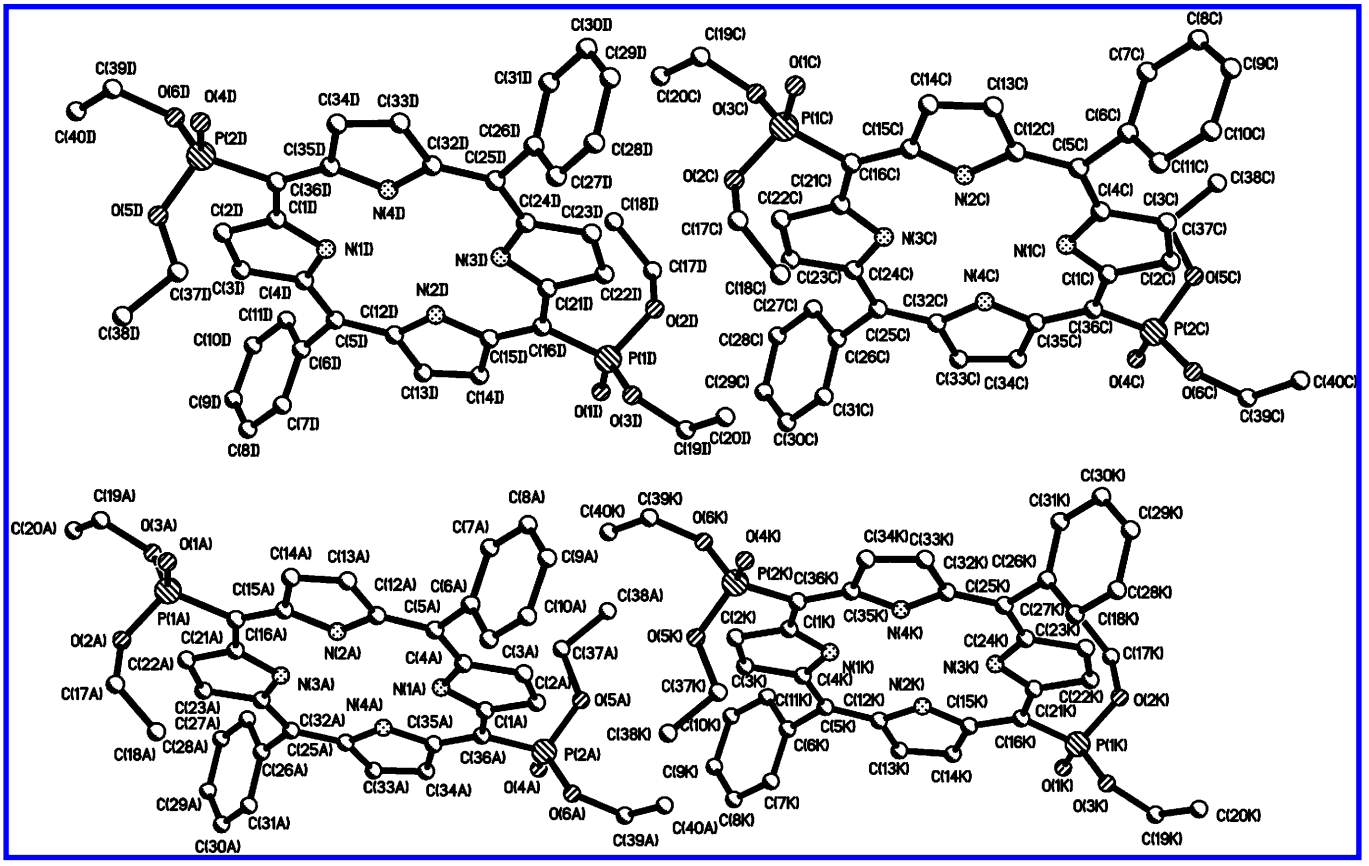

Figure 3. Crystal packing of porphyrin **1**. The hydrogen atoms and solvate molecules of chloroform are omitted for clarity.

dx.doi.org/10.1021/ic302257g | *Inorg. Chem.* XXXX, XXX, XXX−XXX

desorption ionization time-of-flight mass spectrometry (MALDI-TOF MS) and high-resolution electrospray ionization mass spectroscopy (ESI-MS) as well as Fourier transform infrared (FT-IR) spectroscopy (see the Supporting Information).

Surprisingly, the powder X-ray diffraction (XRD) pattern of this polycrystalline sample **3** did not correspond to a simulated pattern for the single-crystal data of **3a**. Dissolving the polycrystalline solid **3** in $CHCl_3$, followed by the addition of hexane and slow evaporation of the solvents, led to the formation of crystals suitable for single-crystal XRD.

According to XRD, the obtained crystals are another polymorphic modification of complex **3** (**3b**; Figure 4 and

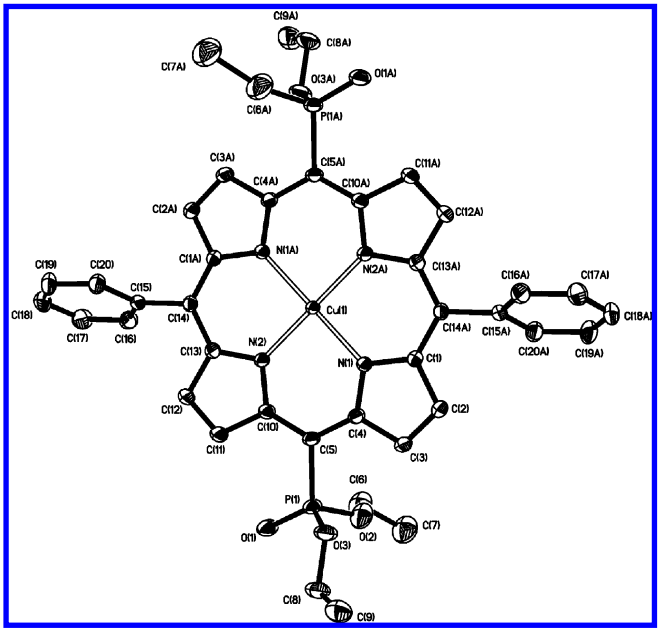

Figure 4. Molecular structure of complex **3b**. Displacement ellipsoids are drawn at the 50% probability level. The hydrogen atoms are omitted for clarity.

Tables S1 and S3 in the Supporting Information). In this case, the simulated pattern from the single-crystal data was found to be in good agreement with the powder XRD patterns of polycrystalline sample **3** (Figure S2 in the Supporting Information).

According to the single-crystal X-ray data of **3b**, the copper atom has a square-planar environment with the four nitrogen atoms of the porphyrin macrocycle; the dihedral angle between the Cu−N(1)−N(2) and Cu−N(1A)−N(2A) planes is equal to 0°; the metal−nitrogen distances Cu(1)−N(1/1A) and Cu(1)−N(2/2A) are 2.0146(16) and 2.0220(15) Å, respectively. These bonds are longer than those of **3a**. The phosphorus atoms of the phosphoryl substituents are almost in the same plane (the displacement of the phosphorus atoms from the CuN_4 plane is ±0.0681 Å). Such a geometry of the copper porphyrin **3b** is probably due to the presence of weak atomic interactions between the oxygen atoms of the phosphoryl group and the copper atom of adjacent porphyrinate [Cu(1/1A)−O(1/1A) = 2.649(3) Å; angle Cu(1A)−P(1)−O(1) = 24.6°]. These interactions lead to the formation of a 2D coordination polymer that is unexpected for copper porphyrins (Figure 5). Similar interactions have been observed in the isostructural zinc porphyrin **2**, but these contacts are much shorter in the zinc complex [Zn(1)−O(1/1A) = 2.487(4) Å; angle Zn(1A)−P(1)−O(1) = 22.0°].[44] The dihedral angles between the planes of the phosphoryl substituents (CP═O) and the porphyrin anion (CCC) change little upon formation of the polymer [C(4)−C(5)−C(10)/C(5)−P(1)−O(1) angle = 4.6° in **3b** and 4.0° in **2**]. The twist angles of the *meso*-phenyl substituents toward the porphyrin plane decrease to 64.3° in **3b** (63.0° in **2**) compared to the free-base porphyrin **1** and the distorted complex **3a** (Figure 4).

The observed interactions between the oxygen atoms of the phosphoryl groups and the metal centers in **3b** and **2** allow us to conclude that, in these structures, the metals have a distorted tetragonal-bipyramidal environment and the porphyrin building blocks form a 2D coordination polymer. Apart from the 1D coordination polymer mentioned in the Introduction,[39] a tetrahydrofuran (THF) solvate of copper(II) tetra(4-pyridyl)-porphyrinate was reported, where the copper ions are formally six-coordinated and ligated by four nitrogen atoms of the porphyrin core and two oxygen atoms of axially coordinated THF molecules [$Cu-O_{THF}$ = 2.81(3) Å].[52]

Thus, copper(II) porphyrin **3** exists in two polymorphic forms, labeled as **a** and **b**. In order to control the formation of a desirable polymorph, the experimental conditions for crystallization of each polymorph were studied (Table 1).

The polycrystalline sample **3b** was dissolved in chloroform, and single crystals suitable for X-ray analysis were grown by the slow diffusion of hexane or methanol, which have opposite polarity and different coordinating properties (Table 1, entries 2 and 3). In both cases, the same single crystals of **3b** were obtained. Slow diffusion of hexane into a chloroform/methanol (1:1) solution of polycrystalline **3b** also led to single crystals of **3b** (Table 1, entry 4).

In an attempt to find the best experimental conditions for obtaining single crystals of **3a** from the polycrystalline sample **3b**, we checked the influence of different parameters on the crystal growth process. In the experiments where polymorph **3a** was obtained, copper(II) acetate was used in excess and acetic acid was formed as a byproduct of the metalation reaction. We tried to simulate these conditions by adding trace amounts of acetic acid or a copper(II) acetate/methanol solution during crystallization. The single crystals were grown by slow diffusion of these solutions into a chloroform solution of copper complex **3** (Table 1, entries 5 and 6). However, the 2D network **3b** was obtained in both cases.

Single crystals of polymorph **3a** could be easily transformed into single crystals of the coordination polymer **3b** by dissolving **3a** in chloroform, followed by consecutive crystallizations, using, for example, slow diffusion of hexane (Table 1, entry 7).

Thus, polymorph **3a** was formed only during slow diffusion of a methanol solution containing copper acetate into a porphyrin **1** solution in chloroform, followed by a simultaneous evaporation of the solvents. It is possible to assume that the growth of crystals **3a** under these conditions is favored because of the low solubility of porphyrin **1** in methanol. The metalation reaction could proceed simultaneously with nucleation and crystal growth under these conditions. These processes lead to formation of the crystals of polymorph **3a**, where the porphyrin backbones are not assembled in the framework similar to the crystals of the free base porphyrin **1**.

The unusual ease of formation of the 2D copper porphyrin network can originate from two factors. One involves the known high affinity of the phosphoryl groups to a metal atom, which could be the driving force of self-assembly. In this case, polymer formation should only be the feature of phosphoryl-substituted

dx.doi.org/10.1021/ic302257g | Inorg. Chem. XXXX, XXX, XXX−XXX

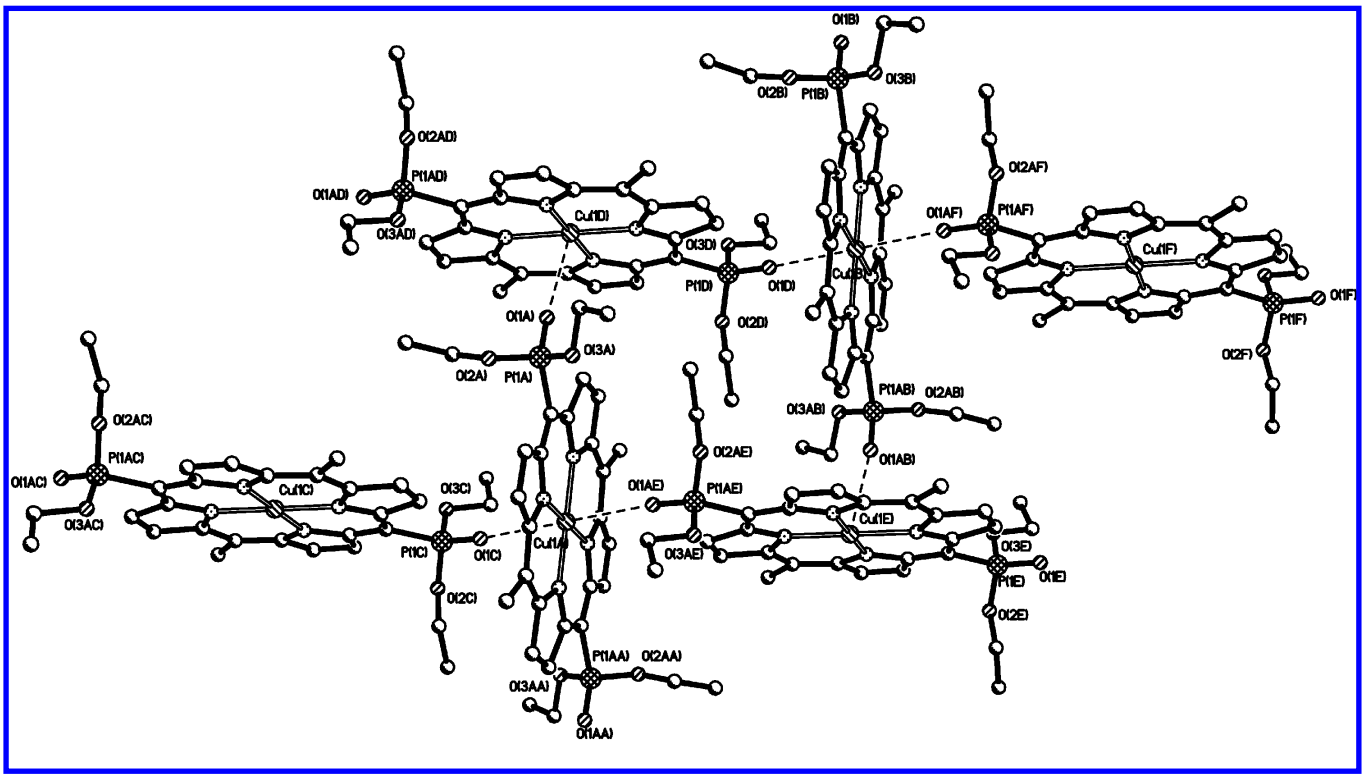

Figure 5. Fragment of crystal packing **3b**. The hydrogen atoms and *meso*-aryl group are omitted for clarity except for the *ipso*-carbon atoms.

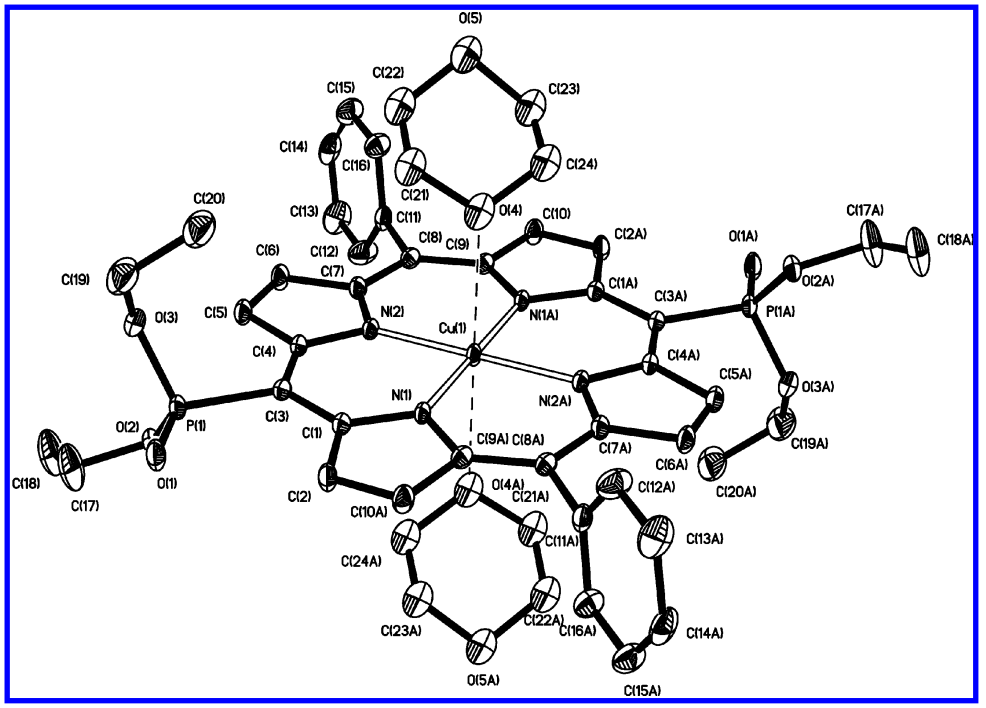

Figure 6. Molecular structure of the dioxane solvate of copper porphyrin complex **3c**. Displacement ellipsoids are drawn at the 50% probability level. The hydrogen atoms are omitted for clarity.

porphyrins. On the other hand, the axial coordination of different coordinating groups could arise from the substantially reduced metal-centered electron density, which is affected by the macrocycle's non-π-conjugating, σ-electron-withdrawing *meso*-phosphoryl substituents. In this case, the self-assembly could be the feature of all electron-deficient porphyrins bearing appropriate coordinating groups. In order to further investigate the influence of these two factors, the interaction of **3** with small coordinating (donor) molecules was studied. Indeed, recrystallization of compound **3** in the presence of dioxane leads to the formation of single crystals of dioxane solvate **3c** (Figure 6, Table 1, entry 8, and Tables S1 and S4 in the Supporting Information).

According to XRD, the copper atom in adduct **3c** has a square-planar environment of four nitrogen atoms [Cu(1)−N(1/1A) =

dx.doi.org/10.1021/ic302257g | *Inorg. Chem.* XXXX, XXX, XXX−XXX

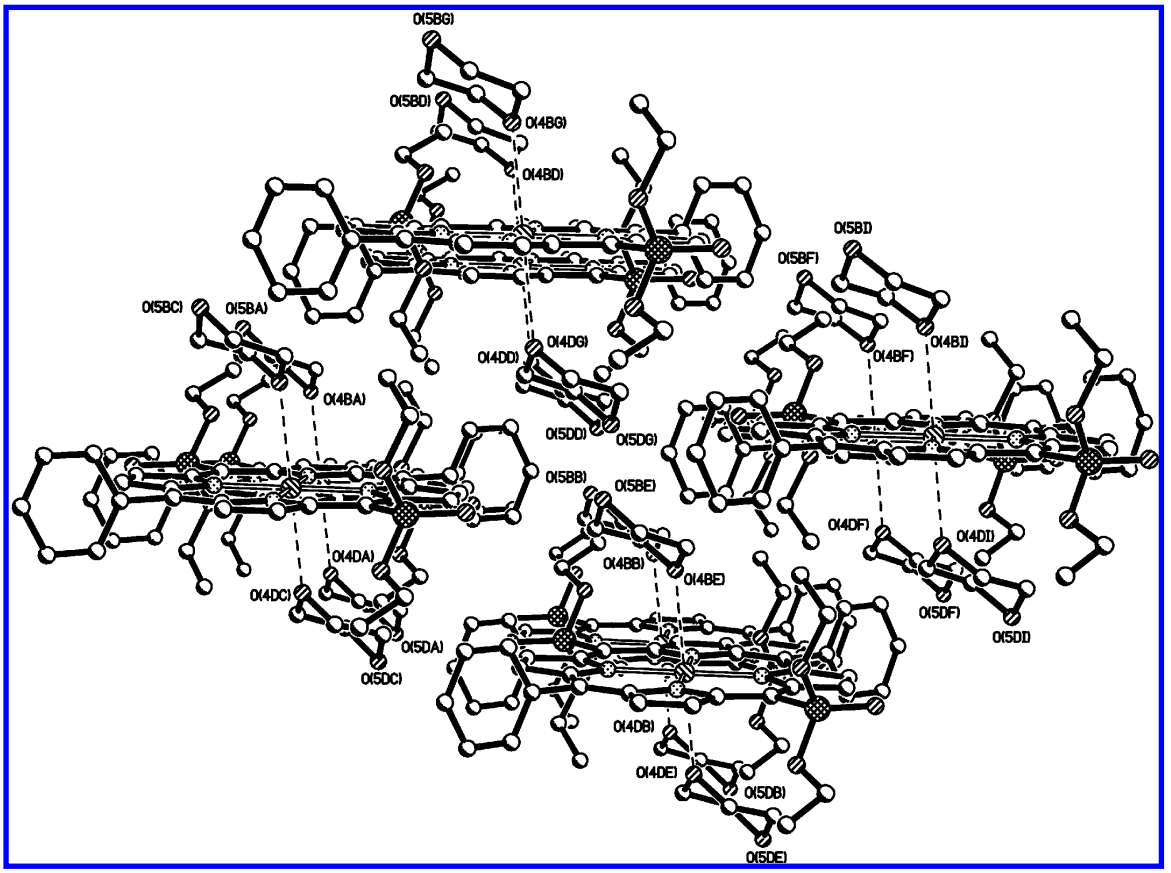

Figure 7. Fragment of the crystal packing of **3c**. The hydrogen atoms are omitted for clarity.

2.017(4) Å; Cu(1)−N(2/2A) = 2.010(3) Å], like in **3b**. Copper has relatively long contacts with the oxygen atoms of the two solvate molecules of dioxane [Cu−O = 2.731(4) Å]. Each of the dioxane molecules is located at an angle of 133.4° [the line O(4)−O(5) with respect to the CuN_4 porphyrin plane].

The porphyrin core is flat [angle Cu−N(1)−N(2)/Cu−N(1A)−N(2A) = 0°], with the phosphorus atoms located above and below the CuN_4 plane and displaced from the plane by ±0.0623 Å. The dihedral angles between the planes of the phenyl substituents and the porphyrin anion are 83.6°. The C(8)−C(11) distance is 1.504(6) Å; the displacements of atoms C(8) and C(11) from the N_4 plane are ±0.057 and ±0.052 Å, respectively. The phosphoryl fragments CP═O are almost in the plane of the porphyrin macrocycle [angle CCC−CP═O = 2.5°, P(1)−C(3) = 1.818(5) Å, P−O(1) = 1.461(4) Å, P−O(2) = 1.564(4) Å, and P−O(3) = 1.593(4) Å]. This strong tendency of the P═O group to be almost in the plane of the porphyrin macrocycle may result from the steric interactions of the ethyl groups as well as the formation of hydrogen bonds between the oxygen atom and the nearest β-hydrogen atom. It should be noted that, in the studied structures (**3a**−**3c**), the distance between the oxygen atom in the P═O group and the nearest β-carbon atom is 2.842−2.863 Å away.

In crystal **3c**, the molecules are bound only by van der Waals interactions (Figure 7) and the donor atoms O(5) in the dioxane solvate molecules do not have any major interactions.

Thus, the presence of strong electron-withdrawing groups directly attached to the porphyrin backbone seems to be the key factor for self-assembly of the investigated copper porphyrin into coordination polymer **3b**.

Self-Assembly of 3 in Solution. The association of porphyrins in a solution can be studied by different spectral techniques, such as, for example, NMR, luminescent, and absorption spectroscopy. The association can also be studied by electrochemical methods. The best choice of spectral instrumentations is dependent on the aggregate nature and stability of the aggregates. Unfortunately, NMR and luminescent spectroscopy are not informative in the case of copper(II) complexes; thus, electron spin resonance (ESR), UV−visible spectroscopy, and cyclic voltammetry were used for this investigation.

The ESR spectrum of **3** in toluene ($c = 6 \times 10^{-3}$ M) at 107.2 K shows a well-defined signal with both copper hyperfine and nitrogen superhyperfine structures (Figure S3 in the Supporting Information). These parameters are typical for copper(II) complexes coordinated by four nitrogen atoms:[53] $g_{II} = 2.203$, $g_{\perp} = 2.060$, $A_{II}^{Cu} = 220 \times 10^{-4}$ cm^{-1}, $A_{\perp}^{N} = 17 \times 10^{-4}$ cm^{-1}, and $A_{II}^{N} = 16 \times 10^{-4}$cm^{-1}. Unfortunately, the sensitivity of ESR spectroscopy to axial aggregate formation in copper(II) complexes is low.[54]

The UV−visible absorption spectra of **1** and **3** in chloroform were also investigated. An intense Soret band is located at 415 nm ($S_0 \rightarrow S_2$ transition) in both compounds. Four less intense Q bands (519, 558, 596, and 650 nm; $S_0 \rightarrow S_1$ transitions) are observed in the spectrum of **1** in chloroform, and these are transformed into two Q bands (553 and 595 nm) after metalation by copper (Figure 8). The shapes and positions of the bands are in good correspondence with previously obtained data for other tetraphenylporphyrins.[55,56] It was earlier shown that UV−visible absorption spectroscopy could be used to estimate the ability of polyphosphorylporphyrin toward self-

dx.doi.org/10.1021/ic302257g | Inorg. Chem. XXXX, XXX, XXX−XXX

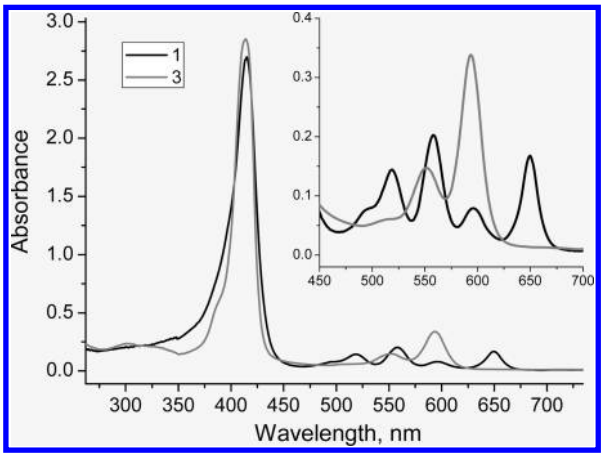

Figure 8. UV−visible absorption spectra of **1** and **3** in chloroform.

assembly in solution.[44,45,57,58] We have investigated the concentration-dependent behavior of copper(II) 5,15-bis-(diethoxyphosphoryl)-10,20-diphenylporphyrinate in toluene and chloroform. Unfortunately, we were unable to see any association of the copper complex in these solvents by means of UV−visible spectroscopy. No evolution of the UV−visible spectrum was observed in toluene over a compound concentration range of 10^{-6}−10^{-3} M or in chloroform over a concentration range of 10^{-5}−10^{-3} M. There is no deviation from Lambert-Beer's law (concentration) in this concentration range in these solvents (Figures S4−S6 in the Supporting Information).

The self-association of **3** was also investigated in solution by means of cyclic voltammetry. The electrochemical properties of complex **3** (c = 10^{-3} M) in PhCN, $CDCl_3$, and CH_2Cl_2 was studied and compared with the properties of complexes **1** and **2** (Table 2 and Figures 9 and 10).

As shown in Table 2 and Figure 9, neutral phosphorylporphyrins **1**−**3** are easier to reduce and harder to oxidize than the corresponding tetraphenylporphyrins with the same central metal ions.[59] These values differ from what has been reported for copper octaethylpophyrins or copper porphyrins substituted with other electron-donating groups.[30,60−62] This is consistent with the effect of the highly electron-withdrawing $P(O)(OEt)_2$ groups on the π-ring systems of **1**−**3**. However, this magnitude of the substituent effect on redox potentials differs as a function of the reaction. For example, when two *meso*-phenyl groups of the tetraphenylporphyrin macrocycles are replaced by two $P(O)(OEt)_2$ groups to form compounds **1**−**3**, the potentials for the first oxidation are positively shifted by 230 mV for all three compounds, while the first reduction potentials are shifted by larger amounts of 360−420 mV (Figure 9). Because a smaller potential shift is seen for the first oxidation, the electrochemical highest occupied molecular orbital (HOMO)−lowest unoccupied molecular orbital (LUMO) gap of the phosphorylporphyrins **1**−**3** in PhCN is less than that of the tetraphenylporphyrin compounds, i.e., 2.03−2.08 V for **1**−**3** compared to 2.16−2.27 V for the related derivatives.

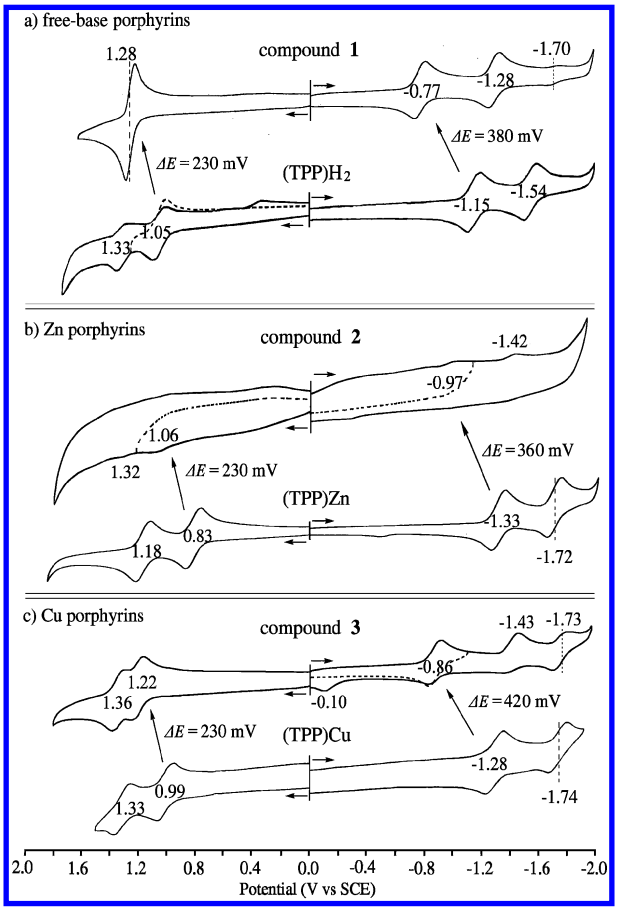

Figure 9. Cyclic voltammograms of porphyrins **1**−**3** and the related tetraphenylporphyrins $TPPH_2$, (TPP)Zn, and (TPP)Cu in PhCN containing 0.1 M TBAP.

Table 2. Half-Wave Potentials (V vs SCE) of the Investigated Phosphorylporphyrins and Related Tetraphenylporphyrins

			oxidation			reduction			
compd	M	solvent	Δox 2-1	2nd ox	1st ox	1st red	2nd red	3rd red	HOMO−LUMO gap
1	2H	PhCN[a]	0	1.28	1.28	−0.77	−1.28	−1.70	2.05
2	Zn		0.26	1.32[b]	1.06	−0.97	−1.42[b]	*c*	2.03
3	Cu		0.14	1.36	1.22	−0.86	−1.43[b]	−1.73	2.08
TPP	2H		0.28	1.33	1.05	−1.15	−1.54		2.20
	Zn		0.35	1.18	0.83	−1.33	−1.72		2.16
	Cu[d]		0.34	1.33	0.99	−1.28	−1.74		2.27
1	2H	$CDCl_3$[e]	0	1.25	1.25	−0.81	−1.40		2.06
2	Zn[f]		0.18	1.18	1.00	−0.99			1.99
3	Cu		0.10	1.36	1.26	−0.90			2.16

[a]Containing 0.1 M TBAP. [b]Peak potential at a scan rate of 0.1 V/s. [c]Not observed due to the poor solubility in PhCN. [d]Data taken from ref 59. [e]Containing 0.2 M TBAP. [f]Data taken from ref 45.

dx.doi.org/10.1021/ic302257g | *Inorg. Chem.* XXXX, XXX, XXX−XXX

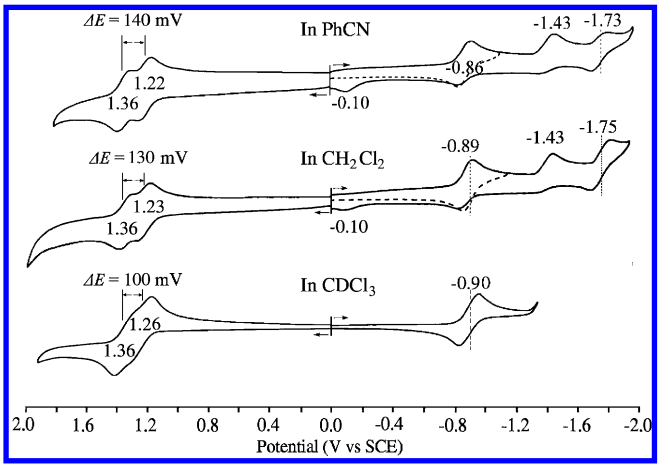

Figure 10. Cyclic voltammograms of **3** ($c = 10^{-3}$ M) in PhCN, CH_2Cl_2, and $CDCl_3$ containing 0.1/0.2 M TBAP.

The introduction of the $P(O)(OEt)_2$ groups onto the porphyrins also leads to a large substituent effect on the second reduction potentials of **1**−**3** (260−310 mV positive shift), while a small effect is seen for the second oxidation (only a 30 mV positive shift occurs in the case of **3**). As a result, the potential difference between the first and second oxidations ($\Delta|ox_2 - ox_1|$) of **1**−**3** is substantially smaller than the corresponding separation for the tetraphenylporphyrins.

The introduction of the $P(O)(OEt)_2$ groups onto porphyrin **1** leads to overlapping of the first and second oxidations (Table 2 and Figure 9). There are many documented examples where the two one-electron oxidations of a porphyrin to give a porphyrin π-cation radical and a dication become overlapped into a single two-electron transfer.[59] This is best known for nickel(II) porphyrins, but it also occurs for some free-base porphyrins. In the current study, the first oxidation is shifted positively by 230 mV from $E_{1/2}$ for oxidation of H_2TPP and the second oxidation is shifted negatively by about 50 mV from the same process of H_2TPP so that both processes overlap, as shown in Figure 9. The fact that the oxidation peak current of **1** at 1.28 V is double that of the reduction at −0.77 V implies an EE mechanism (two one-electron transfers occurring at the same potential) rather than a single two-electron transfer, where the current would increase by $n^{3/2}$.

The separation between the two ring oxidations of **3** is closely related to the self-assembly, as shown previously for related zinc(II) derivatives.[45] In the nonbinding $CHCl_3$ solvent, compound **3** is able to aggregate by the binding of a $P(O)(OEt)_2$ group from one porphyrin molecule to the copper(II) center of another molecule (see Figure 5), while in coordinating solvents, the self-assembly of **3** would be weakened (or blocked) upon axial coordination of the solvent molecules (see Figure 7). Our previous studies of similar zinc porphyrins[45] indicated that the two one-electron oxidations of the self-assembled zinc compounds are always partially overlapped, but these processes were well-separated upon binding with a strong coordinated axial ligand like PPh_3O. This also seems to be the case for compound **3** in CH_2Cl_2 containing added PPh_3O, where the first oxidation shifts negatively by 90 mV from the $E_{1/2}$ value in CH_2Cl_2 containing 0.1 M tetra-*n*-butylammonium perchlorate (TBAP) and the $\Delta E_{1/2}$ between the two oxidation peaks increases from 130 to 190 mV. This is illustrated by the cyclic voltammograms in Figure 11.

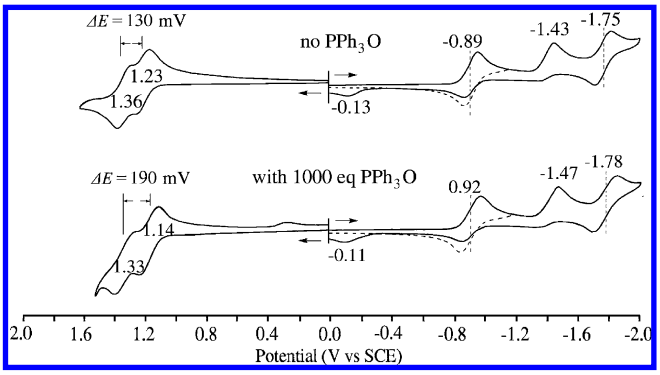

Figure 11. Cyclic voltammograms of copper complex **3** ($c = 10^{-3}$ M) in CH_2Cl_2 containing 0.1 M TBAP with/without PPh_3O.

The $\Delta|ox_2 - ox_1|$ value of **3** is also a function of the solvent binding ability. As shown in Figure 10, the first two reversible oxidations of **3** (at $E_{1/2}$ = 1.26 and 1.36 V) are closely spaced in the nonbinding solvent $CDCl_3$ but are further apart in the bonding solvent PhCN. The value of $\Delta|ox_2 - ox_1|$ for **3** ranges from 140 mV in PhCN to 100 mV in $CDCl_3$, suggesting that the first two oxidations of **3** are affected by the solvent binding, axial coordination in the case of PPh_3O, and aggregation in the nonpolar solvents CH_2Cl_2 and $CDCl_3$. The $\Delta|ox_2 - ox_1|$ value of **3** is also a function of the temperature (Figure S7 in the Supporting Information).

CONCLUSION

In summary, we have described the first example of copper(II) *meso*-phosphorylated porphyrins that exists in the solid state in two polymorphic states: one consists of isolated molecules, and another is the 2D coordination polymer. The unexpected formation of the 2D coordination polymer can be understood if one takes into account the electronic effect of the diethoxyphosphoryl substituents directly attached to the porphyrin core, which modify its coordination properties. Thus, for example, the interaction of copper(II) 5,15-bis(diethoxyphosphoryl)-10,20-diphenylporphyrinate with dioxane molecules also leads to a formally six-coordinated copper(II) ligated by four nitrogen atoms from the porphyrin core and two oxygen atoms of weakly coordinated dioxane molecules. The self-assembly of complex **3** in solution is weak but could be observed by cyclic voltammetry. This process could be prevented or minimized by the use of coordinating solvents, by the addition of coordinating molecules to solution, or by an increase of the temperature of the solution.

Taking into account these results, it is possible to assume that copper−organic frameworks based on porphyrin derivatives should be readily obtained if electron-deficient porphyrins are used as molecular building blocks. The electron-withdrawing nature of the macrocycle peripheral substituents is the key factor of this process, whereas the nature of the axial ligand seems to be less important. Work is now in progress to obtain new examples of copper porphyrin frameworks to prove our conclusion.

EXPERIMENTAL SECTION

Measurements. UV−visible absorption spectra were recorded with a Cary-100 spectrophotometer in quartz cells (1−10 mm). MALDI-TOF MS spectra were recorded on an Ultraflex mass spectrometer (Bruker Daltonics) without a matrix. Accurate mass measurements (high-resolution mass spectrometry) were obtained by ESI on an Orbitrap spectrometer. The measurements were made at the Pôle Chimie Moléculaire, the technological platform for chemical analysis and molecular synthesis (http://www.wpcm.fr), which relies on the

dx.doi.org/10.1021/ic302257g | *Inorg. Chem.* XXXX, XXX, XXX−XXX

Institute of the Molecular Chemistry of University of Burgundy and Welience, a Burgundy University private subsidiary.

IR spectra were registered on a FT-IR Nexus (Nicolet) spectrometer with a micro-ATR accessory (Pike).

ESR spectra were recorded with an ELEXSYS E-680X microwave spectrometer (Bruker). The powder XRD patterns were measured in Bragg−Brentano mode using an EMPYREAN (PANalytical) diffractometer (Cu Kα_1 radiation; λ = 1.54059 Å; tube voltage/current 45 kV/40 mA) with a linear X'celerator detector at ambient conditions [T = 295(2) K]. The data collection region was 2θ = 3−30° with a step of 0.008° and 50 s/step in continuous mode. Samples suspended in hexane were dropped onto a zero-background-oriented plate (silicon, single crystal), and after evaporation of the solvent, the powder XRD pattern was measured.

XRD data collection was carried out on a Bruker SMART APEX II CCD detector with λ(Mo Kα) = 0.71073 Å, a graphite monochromator, ω scanning, and $2\theta_{max}$ = 56°. Diffraction data sets were corrected for absorption using *SADABS*.[63] Structures were solved by direct methods and refined by a full-matrix least-squares method for F^2 with anisotropic parameters for all non-hydrogen atoms. All calculations were performed by means of the *SAINT*[64] and *SHELXTL-97*[65] program packages. CCDC reference numbers are 902785−902787. The data can be obtained free of charge from the Cambridge Crystallographic Data Centre at www.ccdc.cam.ac.uk/data_request/cif.

Synthesis. All chemicals used were of analytical grade and were purchased from Acros and Sigma-Aldrich Co. Chloroform was dried over anhydrous $CaCl_2$, followed by distillation over CaH_2. Methanol was dried over 4 Å molecular sieves. Silica gel (0.04−0.063 mm; 230−400 mesh; ASTM, Merck) was used for column chromatography. The free base 5,15-bis(diethoxyphosphoryl)-10,20-diphenylporphyrin was synthesized according to previously published methods.[44,45]

Synthesis of Copper(II) 5,15-Bis(diethoxyphosphoryl)-10,20-diphenylporphyrinate (3). Copper(II) acetate hydrate (14.6 mg, 0.07 mmol) in 0.25 mL of CH_3OH was added to a solution of 5,15-bis(diethoxyphosphoryl)-10,20-diphenylporphyrin (15.2 mg, 0.02 mmol) in a 3 mL mixture of $CHCl_3$ and CH_3OH (10:1). The mixture was stirred at room temperature for 30 min and the solvent removed under reduced pressure. The violet precipitate was dissolved in $CHCl_3$ and chromatographed on silica gel. The compound was eluted with $CHCl_3$. Slow evaporation of this solution in air yielded crystalline compound **3** (15 mg, 91%). UV−visible [toluene; λ_{max}, nm (ε, dm^3 mol^{-1} cm^{-1})]: 413 (3.75×10^5), 543 (1.44×10^4), 585 (3.14×10^4). UV−visible [chloroform; λ_{max}, nm (ε, dm^3 mol^{-1} cm^{-1})]: 415 (2.59×10^5), 553 (1.05×10^4), 595 (2.61×10^4). MALDI-TOF MS: m/z 796.9 (exptl); m/z 796.3 (theor). HRMS: m/z 818.14383 (exptl, [M + Na]$^+$); m/z 818.14548 (theor, [M + Na]$^+$). EPR spectrum (toluene, $c = 6 \times 10^{-3}$ mol/L, 107.2 K): g_{II} = 2.203, $g_\perp$ = 2.060, $A_{II}^{Cu} = 220 \times 10^{-4}$ cm^{-1}, $A^N = 17 \times 10^{-4}$ cm^{-1}, and $A_{II}^N = 16 \times 10^{-4}$ cm^{-1}.

Powder XRD analysis of the solid: monoclinic, a = 12.314(2) Å, b = 11.808(1) Å, c = 12.449(1) Å, and β = 91.814 (9)°.

Crystal Growth. Single crystals of **3a** suitable for X-ray analysis were obtained by slow diffusion of a 1 mL of copper(II) acetate hydrate solution in MeOH ($c = 5.08 \times 10^{-3}$ M) into a solution (1 mL) of the free-base porphyrin **1** in $CHCl_3$ ($c = 1.27 \times 10^{-3}$ M) in reagent ratio 1:1 or 4:1. The experiment was performed at room temperature in tubes without lids. Violet single crystals of **3a** suitable for X-ray analysis were obtained in both cases.

Single crystals of **3b** suitable for X-ray analysis were obtained at room temperature by the slow diffusion of hexane (1 mL) to a chloroform solution of polycrystalline compound **3** (1 mL, 3×10^{-3} M).

Single crystals of **3c** suitable for X-ray analysis were obtained by slow evaporation of a solution of **3b** in dioxane (2 mL, 3×10^{-3} M).

Crystallization of 3b in Different Conditions. (a) A solution of **3b** in chloroform (1 mL, 3×10^{-3} M) was placed in a glass tube. Hexane (1 mL) was added to the tube as an upper layer, and the tube was left at room temperature without the lid for 3 days. Single crystals of **3b** suitable for X-ray analysis were obtained by the slow evaporation of solvents.

(b) A solution of **3b** in chloroform (1 mL, 3×10^{-3} M) was put in the glass tube, and methanol (1 mL) was added to the tube as an upper layer. The tube with the lid was left in the refrigerator (T = 4 °C) for 5 days, and then the tube was left at room temperature without the lid for 9 days. Single crystals of **3b** suitable for X-ray analysis were obtained by the slow evaporation of solvents.

(c) A solution of **3b** in a mixture of chloroform and methanol (2 mL, 3×10^{-3} M, solvent ratio 1:1) was put in the glass tube, and the same volume of hexane was added to the tube as an upper layer. The tube with the lid was left in the refrigerator (T = 4 °C) for 9 days, after which single crystals of **3b** suitable for X-ray analysis were obtained by slow diffusion.

(d) A solution of **3b** in chloroform (1 mL, 3×10^{-3} M) was put in a glass tube, and methanol with a trace of CH_3COOH (1 drop of CH_3COOH in 500 μL of methanol) was added to the tube as an upper layer. The tube with the lid was left in the refrigerator (T = 4 °C) for 5 days, after which the lid was removed and the tube was left at room temperature for 9 days. Single crystals of **3b** suitable for X-ray analysis were obtained by the slow evaporation of solvents.

(e) A solution of **3b** in chloroform (1 mL, 3×10^{-3} M) was put in the glass tube, and the copper(II) acetate hydrate solution in MeOH (1 mL, $c = 5.08 \times 10^{-3}$ M) was added to the tube as an upper layer. The tube was left at room temperature without a lid for 2 weeks. Single crystals of **3b** suitable for X-ray analysis were obtained by the slow evaporation of solvents.

(f) Single crystals of **3a** were dissolved in chloroform (1 mL). Hexane (1 mL) was added to the tube as an upper layer, and the tube then was left at room temperature without a lid for 3 days. Single crystals of **3b** suitable for X-ray analysis were obtained by the slow evaporation of solvents.

Electrochemical Measurements. Cyclic voltammetry was carried out with an EG&G model 173 potentiostat/galvanostat. A homemade three-electrode cell was used and consisted of a platinum button or glassy carbon working electrode, a platinum wire counter electrode, and a saturated calomel reference electrode (SCE). The SCE was separated from the bulk of the solution by a fritted-glass bridge of low porosity, which contained the solvent/supporting electrolyte mixture. All potentials are referenced to the SCE (+0.2444 V vs NHE at 25 °C).

TBAP (≥99%) was purchased from Fluka Chemical Co., recrystallized from ethyl alcohol, and dried under vacuum at 40 °C for at least 1 week prior to use. Absolute dichloromethane (CH_2Cl_2; 99.8%, EMD Chemical Inc.) and chloroform-*d* ($CDCl_3$; 99.8+% isotopic, Alfa. Aesar Co.) were used as received. Benzonitrile (PhCN; 99%, Aldrich Co.) was distilled over phosphorus pentoxide (P_2O_5) under vacuum prior to use.

■ ASSOCIATED CONTENT

Supporting Information

X-ray crystallographic files in CIF format for **3a**, **3b**, and **3c**, powder XRD experiment, spectral and electrochemical data. This material is available free of charge via the Internet at http://pubs.acs.org.

■ AUTHOR INFORMATION

Corresponding Author

*E-mail: yulia@igic.ras.ru (Y.G.G.), Roger.Guilard@u-bourgogne.fr (R.G.).

Notes

The authors declare no competing financial interest.

■ ACKNOWLEDGMENTS

This work was performed in the frame of the French−Russian Associated Laboratory "LAMREM" supported by the CNRS and Russian Academy of Sciences, Russian Foundation for Basic Research (Grant 12-03-93110). The authors thank Prof. V. V. Minin and Dr. N. N. Efimov for EPR experiments and Dr. A. A. Shiryaev with Prof. V. V. Chernyshov for help with powder XRD experiments. Support from the Robert A. Welch Foundation (to K.M.K.; Grant E-680) is also gratefully acknowledged.

REFERENCES

(1) Wasielewski, M. R. *Acc. Chem. Res.* **2009**, *42*, 1910.
(2) Elliott, K. J.; Harriman, A.; Le Pleux, L.; Pellegrin, Y.; Blart, E.; Mayer, C. R.; Odobel, F. *Phys. Chem. Chem. Phys.* **2009**, *11*, 8767.
(3) Balaban, T. S. In *Handbook of Porphyrin Science*; Kadish, K. M., Smith, K. M., Guilard, R., Eds.; World Scientific Publishing Co. Pte. Ltd.: Singapore, 2010; Vol. *1*, pp 221−306.
(4) Panda, M. K.; Ladomenou, K.; Coutsolelos, A. G. *Coord. Chem. Rev.* **2012**, *256*, 2601.
(5) Filatov, M. A.; Laquai, F.; Fortin, D.; Guilard, R.; Harvey, P. D. *Chem. Commun.* **2010**, *46*, 9176.
(6) Harvey, P. D.; Filatov, M. A.; Guilard, R. *J. Porphyrins Phthalocyanines* **2011**, *15*, 1150.
(7) Szmytkowski, J.; Conradt, J.; Kuhn, H.; Reddy, C. M.; Balaban, M. C.; Balaban, T. S.; Kalt, H. *J. Phys. Chem. C* **2011**, *115*, 8832.
(8) Camus, J.-M.; Aly, S. M.; Stern, C.; Guilard, R.; Harvey, P. D. *Chem. Commun.* **2011**, *47*, 8817.
(9) Liu, J.-Y.; El-Khouly, M. E.; Fukuzumi, S.; Ng, D. K. P. *Chem.—Eur. J.* **2011**, *17*, 1605.
(10) Beletskaya, I.; Tyurin, V. S.; Tsivadze, A. Y.; Guilard, R.; Stern, C. *Chem. Rev.* **2009**, *109*, 1659.
(11) Chambron, J.-C.; Heitz, V.; Sauvage, J.-P. In *The Porphyrin Handbook*; Kadish, K. M., Smith, K. M., Guilard, R., Eds.; Academic Press: San Diego, CA, 2000; Vol. *6*, pp 1−42.
(12) Drain, C. M.; Varotto, A.; Radivojevic, I. *Chem. Rev.* **2009**, *109*, 1630.
(13) DeVries, L. D.; Choe, W. *J. Chem. Crystallogr.* **2009**, *39*, 229.
(14) Aratani, N.; Kim, D.; Osuka, A. *Acc. Chem. Res.* **2009**, *42*, 1922.
(15) Aratani, N., Osuka, A. In *Handbook of Porphyrin Science*; Kadish, K. M., Smith, K. M., Guilard, R., Eds.; World Scientific Publishing Co. Pte. Ltd.: Singapore, 2010; Vol. *1*, pp 1−132.
(16) Ding, X.; Feng, X.; Saeki, A.; Seki, S.; Nagai, A.; Jiang, D. *Chem. Commun.* **2012**, *48*, 8952.
(17) Alessio, E.; Casanova, M.; Zangrando, E.; Iengo, E. *Chem. Commun.* **2012**, *48*, 5112.
(18) Ikeda, S.; Aratani, N.; Osuka, A. *Chem. Commun.* **2012**, *48*, 4317.
(19) Shmilovits, M.; Diskin-Posner, Y.; Vinodu, M.; Goldberg, I. *Cryst. Growth Des.* **2003**, *3*, 855.
(20) Vinodu, M.; Stein, Z.; Goldberg, I. *Inorg. Chem.* **2004**, *43*, 7582.
(21) Kuhn, E.; Bulach, V.; Hosseini, M. W. *Chem. Commun.* **2008**, 5104.
(22) Kojima, T.; Honda, T.; Ohkubo, K.; Shiro, M.; Kusukawa, T.; Fukuda, T.; Kobayashi, N.; Fukuzumi, S. *Angew. Chem., Int. Ed.* **2008**, *47*, 6712.
(23) Mizumura, M.; Shinokubo, H.; Osuka, A. *Angew. Chem., Int. Ed.* **2008**, *47*, 5378.
(24) Choi, E. Y.; Barron, P. M.; Novotny, R. W.; Son, H. T.; Hu, C.; Choe, W. *Inorg. Chem.* **2008**, *48*, 426.
(25) Moustakali, I.; Tulinsky, A. *J. Am. Chem. Soc.* **1973**, *95*, 6811.
(26) Renner, M. W.; Barkigia, K. M.; Zhang, Y.; Medforth, C. J.; Smith, K. M.; Fajer, J. *J. Am. Chem. Soc.* **1994**, *116*, 8582.
(27) Senge, M. O.; Bischoff, I.; Nelson, N. Y.; Smith, K. M. *J. Porphyrins Phthalocyanines* **1999**, *3*, 99.
(28) McGhee, E. M.; Godfrey, M. R.; Hoffman, B. M.; Ibers, J. A. *Inorg. Chem.* **1991**, *30*, 803.
(29) Jiao, L.; Courtney, B. H.; Fronczek, F. R.; Smith, K. M. *Tetrahedron Lett.* **2006**, *47*, 501.
(30) Chen, W.; El-Khouly, M. E.; Fukuzumi, S. *Inorg. Chem.* **2011**, *50*, 671.
(31) Chen, W.; Fukuzumi, S. *Eur. J. Inorg. Chem.* **2009**, *4*, 5494.
(32) Deiters, E.; Bulach, V.; Hosseini, M. W. *New J. Chem.* **2008**, *32*, 99.
(33) Deiters, E.; Bulach, V.; Hosseini, M. W. *New J. Chem.* **2006**, *30*, 1289.
(34) Zimmer, B.; Bulach, V.; Hosseini, M. W.; De Cian, A.; Kyritsakas, N. *Eur. J. Inorg. Chem.* **2002**, *2002*, 3079.
(35) Hagrman, D.; Hagrman, P.; Zubieta, J. *Angew. Chem., Int. Ed.* **1999**, *38*, 3165.
(36) Muniappan, S.; Lipstman, S.; George, S.; Goldberg, I. *Inorg. Chem.* **2007**, *46*, 5544.
(37) Lipstman, S.; Muniappan, S.; George, S.; Goldberg, I. *Dalton Trans.* **2007**, 3273.
(38) Wang, X.-S.; Meng, L.; Cheng, Q.; Kim, C.; Wojtas, L.; Chrzanowski, M.; Chen, Y.-S.; Zhang, X. P.; Ma, S. *J. Am. Chem. Soc.* **2011**, *133*, 16322.
(39) Zimmer, B.; Hutin, M.; Bulach, V.; Hosseini, M. W.; De Cian, A.; Kyritsakas, N. *New J. Chem.* **2002**, 1532.
(40) Lippard, S. J.; Berg, J. M. *Principles of Bioinorganic Chemistry*; University Science Books: Mill Valley, CA, 1994.
(41) Zeng, J.; Xia, Y. *Nat. Nano* **2012**, *7*, 415.
(42) Murase, S.; Ishino, S.; Ishino, Y.; Tanaka, T. *J. Biol. Inorg. Chem.* **2012**, *17*, 791.
(43) Cao, R.; Müller, P.; Lippard, S. J. *J. Am. Chem. Soc.* **2010**, *3*, 17366.
(44) Enakieva, Y. Y.; Bessmertnykh, A. G.; Gorbunova, Y. G.; Stern, C.; Rousselin, Y.; Tsivadze, A. Y.; Guilard, R. *Org. Lett.* **2009**, *11*, 3842.
(45) Kadish, K. M.; Chen, P.; Enakieva, Y. Y.; Nefedov, S. E.; Gorbunova, Y. G.; Tsivadze, A. Y.; Bessmertnykh-Lemeune, A.; Stern, C.; Guilard, R. *J. Electroanal. Chem.* **2011**, *656*, 61.
(46) Rao, V. M.; Sathyanarayana, D. N.; Manohar, H. *J. Chem. Soc., Dalton Trans.* **1983**, 2167.
(47) Fleischer, E. B. *J. Am. Chem. Soc.* **1963**, *85*, 1353.
(48) Tsai, C.-H.; Tung, J.-Y.; Chen, J.-H.; Liao, F.-L.; Wang, S.-L.; Wang, S.-S.; Hwang, L.-P.; Chen, C.-B. *Polyhedron* **2000**, *19*, 633.
(49) Goldberg, I.; Krupitsky, H.; Stein, Z.; Hsiou, Y.; Strouse, C. E. *Supramol. Chem.* **1994**, *4*, 203.
(50) He, H.-S. *Acta Crystallogr., Sect. E* **2007**, *63*, m976.
(51) Konarev, D. V.; Neretin, I. S.; Slovokhotov, Y. L.; Yudanova, E. I.; Drichko, N. V.; Shul, M.; Tarasov, B. P.; Gumanov, L. L.; Batsanov, A. S.; Howard, J. A. K.; Lyubovskaya, R. N. *Chem.—Eur. J.* **2001**, *7*, 2605.
(52) Wang, J.-Q.; Ren, C.-X.; Weng, L.-H.; Jin, G.-X. *Chem. Commun.* **2006**, 162.
(53) Eaton, S. S.; Eaton, G. R.; Chang, C. K. *J. Am. Chem. Soc.* **1985**, *107*, 3177.
(54) Andersson, K. K.; Schmidt, P. P.; Katterle, B.; Strand, K. R.; Palmer, A. E.; Lee, S. K.; Solomon, E. I.; Gräslund, A.; Barra, A. L. *J. Biol. Inorg. Chem.* **2003**, *8*, 235.
(55) Pekkarinen, L.; Linschitz, H. *J. Am. Chem. Soc.* **1960**, *82*, 2407.
(56) Drouet, S.; Paul-Roth, C. O.; Simonneaux, G. *Tetrahedron* **2009**, *65*, 2975.
(57) Matano, Y.; Matsumoto, K.; Terasaka, Y.; Hotta, H.; Araki, Y.; Ito, O.; Shiro, M.; Sasamori, T.; Tokitoh, N.; Imahori, H. *Chem.—Eur. J.* **2007**, *13*, 891.
(58) Atefi, F.; McMurtrie, J. C.; Arnold, D. P. *Dalton Trans.* **2007**, 2163.
(59) Kadish, K. M.; Van Caemelbecke, E.; Royal, G. In *The Porphyrin Handbook*; Kadish, K. M., Smith, K. M., Guilard, R., Eds.; Academic Press: San Diego, 2000; Vol. *8*, pp 1−114.
(60) Fuhrhop, J.-H.; Kadish, K. M.; Davis, D. G. *J. Am. Chem. Soc.* **1973**, *95*, 5140.
(61) Sibilia, S. A.; Hu, S.; Piffat, C.; Melamed, D.; Spiro, T. G. *Inorg. Chem.* **1997**, *36*, 1013.
(62) Bhyrappa, P.; Krishnan, V. *Inorg. Chem.* **1991**, *30*, 239.
(63) Sheldrick, G. M. *SADABS*; Bruker AXS Inc.: Madison, WI, 1997.
(64) *SMARTV5.051 and SAINTV5.00, Area detector control and integration software*; Bruker AXS Inc.: Madison, WI, 1998.
(65) Sheldrick, G. M. *SHELXTL-97V5.10*; Bruker AXS Inc.: Madison, WI, 1997.